The effect of hydrodynamic interactions on the average properties of a bidisperse suspension of high Reynolds number, low Weber number bubbles

V. Kumaran and Donald L. Koch
School of Chemical Engineering, Cornell University, Ithaca, New York 14853

The hydrodynamic interaction between a pair of nondeformable bubbles (low Weber number limit) in potential flow (high Reynolds number limit) was analyzed. The velocity potential was determined using twin spherical expansions, and the equations of motion were calculated by enforcing the zero net force condition on the surface of the bubbles. The acceleration due to the interaction is expressed in a perturbation series in the parameter (a_i/R), where a_i is the radius of bubble i, R is the distance between the bubbles, and the leading-order acceleration was found to decrease as $(a_i/R)^4$. The effect of potential flow interactions on the trajectory of a pair of bubbles of different sizes (size ratio greater than 1.07 at a Reynolds number of 200) rising due to gravity was studied. A salient feature of the trajectories is that the surfaces of the bubble do not come into contact during the interaction, except when the smaller bubble radius is less than 0.233 times the larger bubble radius when the Reynolds number based on the larger bubble is 200. In the latter case, however, the Reynolds number based on the radius of the smaller bubble is not large enough to justify the potential flow approximation. For interactions where collisions do not occur, the mean-square fluctuating velocity in a uniform suspension and the hydrodynamic diffusivities in a nonuniform suspension were calculated by performing an ensemble average over pair interactions. The pair averaging procedure is valid for dilute suspensions ($V \ll 18/\mathrm{Re}$, where V is the volume fraction of the bubbles and Re is the Reynolds number based on the bubble radius and its terminal velocity).

I. INTRODUCTION

In this paper, we study the dynamics of a suspension of bubbles in the high Reynolds number, low Weber number limit. For air bubbles of diameter 0.4–0.8 mm rising in water, the Reynolds number, $\mathrm{Re} = \rho U_0 a / \eta$, varies between 50 and 350 and the Weber number, $\mathrm{We} = \rho U_0^2 a / \gamma$, varies between 7.6×10^{-4} and 2. Here ρ and η are the fluid density and viscosity, a is the bubble radius, U_0 is a characteristic velocity, and γ is the surface tension. This limit is of interest even though it only occurs for a small range of bubble sizes because the analysis of bubble interactions is sufficiently simple that the average properties of a suspension can be investigated in some detail.

The motion of a single bubble under high Reynolds number and low Weber number conditions has been studied extensively. In the absence of surfactants, there is a slip boundary condition at the surface of the bubble due to the small viscosity of the gas. It has been shown (Moore[1] and Levich[2]) that the flow around the bubble is inviscid and irrotational to leading order, and the correction to this base flow is $O(\mathrm{Re}^{-1/2})$ in the boundary layer and wake. The boundary layer has a thickness of $O(\mathrm{Re}^{-1/2})$, and the wake has a thickness of $O(\mathrm{Re}^{-1/4})$ smaller than the bubble radius. In the limit of high Reynolds number, the flow around the bubble is adequately described by the potential flow approximation. The deformation of a rising bubble under low Weber number conditions was examined by Moore.[3] Assuming that the shape of the bubble is an oblate spheroid, Moore found that the ratio of the major and minor axes is $(1 + \frac{9}{32}\mathrm{We})$. Numerical studies by Ryskin and

Leal[4] showed that the bubble deformation is small when the Weber number is less than about 2. For Weber numbers greater than 4, boundary-layer separation occurs and the potential flow approximation is no longer valid.

The interactions between nondeformable bubbles were analyzed by Biesheuvel and van Wijngaarden,[5] who used the method of twin spherical expansions to calculate the velocity potential in the absence of external forces. The bubbles were originally at rest in a container of liquid in the absence of external forces, and this container was instantaneously accelerated to a finite velocity. The zero net force condition was enforced using Lagally's theorem, and the equation for the bubble accelerations were derived. The authors recently became aware of a theoretical study of the interaction between a pair of equal sized bubbles by Kok.[6,7] In this analysis, the equations of motion were calculated using an energy balance formulation, and the interaction between a pair of equal sized bubbles rising due to gravity was studied.

The interaction between a pair of nondeformable bubbles in potential flow is analyzed in Sec. II. The velocity potential is calculated using the method of twin spherical expansions, which was earlier used to study the interactions between equal sized bubbles in the absence of external forces by Biesheuvel and van Wijngaarden.[5] The present analysis is more general, however, and we describe the interaction between a pair of bubbles of different sizes in the presence of external forces. The equation for the acceleration of the bubbles is derived as an asymptotic series in (a_i/R). Here a_i, for $i=1$ and 2, are the radii of the bubbles

and R is the distance between the centers of the bubbles. The Bernoulli equation, which is used to calculate the pressure on the surface of the bubble, is a nonlinear equation, and is explicitly dependent on time. This makes the analysis of bubble interactions more difficult than the analysis of interactions between low Reynolds number particles, which are described by the linear and quasisteady Stokes equations. However, the calculation of average properties is simpler in the present case, because the leading-order acceleration decreases as $(1/R)^4$, and therefore we do not encounter divergent integrals.

The result of an interaction between a pair of bubbles rising due to gravity in potential flow depends on the ratio of the bubble sizes. The interaction between bubbles of nearly equal size (radius ratios between 0.93 and 1.07 at Re=200) is analyzed in Kumaran and Koch.[8] In this case, the bubbles approach each other along the horizontal plane and collide. If we assume that the result of the initial collision is an elastic bounce, the bubbles collide repeatedly thereafter. The amplitude of the oscillations decreases due to viscous drag, and the bubbles rise as a horizontally aligned pair. Based on the scaling of the pressure and velocity fields in the small gap, we expect coalescence to occur. The frequency of coalescence in a dilute suspension of bubbles is calculated by doing an ensemble average over pair interactions.

For larger size ratios, the surfaces of the bubbles do not come into contact during an interaction, so the possibility of coalescence does not arise. In Sec. III, we use the potential flow solution from Sec. II to analyze this type of interaction. The mean and mean-square velocities and the hydrodynamic diffusivities of bubbles in a bidisperse suspension are calculated in Sec. IV. Most previous treatments of the average behavior of bubble suspensions have not included any detailed description of bubble interactions (see, for example, Drew[9] and Wallis[10]). Studies that have included hydrodynamic bubble interactions have generally focused on the concentration dependence of the added mass or drag coefficient in a static array of bubbles (van Wijngaarden and Biesheuvel,[11] Kok,[6] and Sangani et al.[12]). By including the bubble dynamics, we are able to determine the variance of the bubble velocity and the bubble's hydrodynamic diffusivity as well as the changes in the mean velocity.

II. POTENTIAL FLOW INTERACTIONS BETWEEN NONDEFORMABLE BUBBLES

The problem configuration consists of two spherical bubbles of radii a_1 and a_2, which are centered at positions x_1 and x_2 and have velocities U_1 and U_2 as shown in Fig. 1. The velocity of the fluid u is expressed as the gradient of the velocity potential ϕ:

$$u = \nabla \phi. \tag{1}$$

The velocity potential satisfies the Laplace equation:

$$\nabla^2 \phi = 0. \tag{2}$$

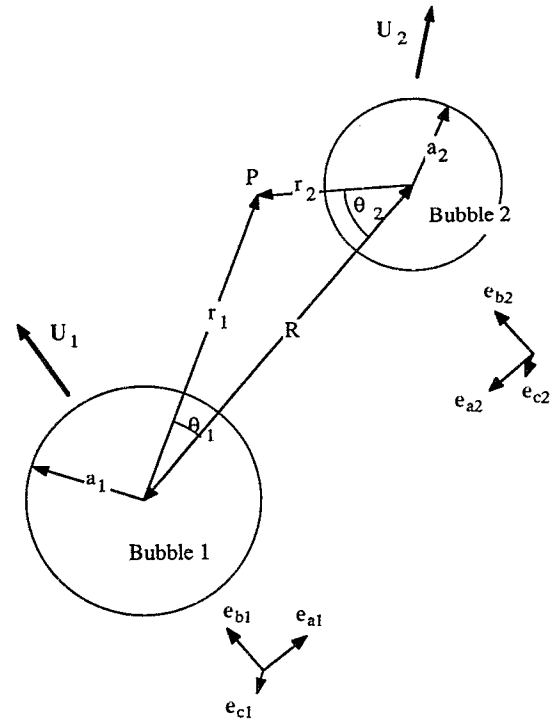The liquid pressure is given by the Bernoulli equation:

FIG. 1. Definition of coordinate system for analyzing the interactions between nondeformable bubbles.

$$\frac{p}{\rho} = -\frac{\partial \phi}{\partial t} - \frac{1}{2} u^2. \tag{3}$$

The bubbles are not deformable, so the velocity of the fluid normal to the surface of the bubble is equal to the velocity of the bubble in that direction,

$$u \cdot n = U_i \cdot n. \tag{4}$$

Since the gas density is $O(10^{-3})$ smaller than the density of the liquid, we assume that the mass of the bubble is zero and therefore the net force acting on the bubble is zero,

$$-\int_{A_i} p n_i \, dA_i + F_i = 0. \tag{5}$$

Here A_i is the surface of bubble i, n_i is the outward unit normal to the surface, and F_i is the sum of the external forces on the bubble. In addition to the above conditions, the fluid velocity and pressure are zero at large distances from the bubble. Equations (1)–(5) are solved to calculate the acceleration of the bubbles due to interactions.

To simplify the analysis, we express the velocities of the bubbles in terms of the common velocity V and the difference velocity W:

$$V = \tfrac{1}{2}(U_1 + U_2), \tag{6a}$$

$$W = \tfrac{1}{2}(U_1 - U_2). \tag{6b}$$

The coordinate systems used in analyzing this problem are shown in Fig. 1. A Cartesian coordinate system fixed in the stationary frame tracks the absolute displacement of the bubbles in space. In addition we use two spherical coordi-

nate systems at the centers of the bubbles. Here e_{ai} is the unit vector directed from the center of bubble i to the center of the other bubble $(3-i)$, and serves as the axis for the spherical coordinates. The two unit vectors perpendicular to this axis are e_{bi} and e_{ci}. Note that e_{a1} and e_{a2} are opposite in direction to each other, whereas the other two unit vectors are in the same direction. The radial and the azimuthal coordinates in the coordinate system centered at bubble i are r_i and θ_i, respectively, and the common meridional angle for the two systems is μ. The relations between the unit vectors in the spherical and Cartesian coordinate systems are

$$e_{ri} = \cos\theta_i\, e_{ai} + \sin\theta_i \cos\mu\, e_{bi} + \sin\theta_i \sin\mu\, e_{ci}, \quad (7a)$$

$$e_{qi} = -\sin\theta_i\, e_{ai} + \cos\theta_i \cos\mu\, e_{bi} + \cos\theta_i \sin\mu\, e_{ci}, \quad (7b)$$

$$e_\mu = -\cos\mu\, e_{bi} + \sin\mu\, e_{ci}. \quad (7c)$$

The velocity potential is expressed as a function of the bubble velocities and separation using the method of twin spherical expansions. Since the Laplace equation and the boundary conditions are linear, the velocity potentials ϕ_{Vk} and ϕ_{Wk}, driven by the components of the common and difference velocities V_k and W_k in the three directions ($k = a,b,c$) can be evaluated independently and then superimposed to give the velocity potential. The Laplace equation is solved in spherical coordinates using the method of separation of variables. Since the velocity of the fluid decreases to zero at large distances from the bubbles, only the decaying harmonics are retained. The solutions for the contributions to the velocity potential are

$$\phi_{Vk} = \sum_{n=1}^{\infty} V_k a_1 \left[g_{mn}^1 \left(\frac{a_1}{r_1}\right)^{n+1} Y_n^k(\theta_1,\mu) \right.$$
$$\left. + g_{mn}^2 \left(\frac{a_2}{r_2}\right)^{n+1} Y_n^k(\theta_2,\mu) \right], \quad (8)$$

$$\phi_{Wk} = \sum_{n=1}^{\infty} W_k a_1 \left[f_{mn}^1 \left(\frac{a_1}{r_1}\right)^{n+1} Y_n^k(\theta_1,\mu) \right.$$
$$\left. + f_{mn}^2 \left(\frac{a_2}{r_2}\right)^{n+1} Y_n^k(\theta_2,\mu) \right], \quad (9)$$

where

$$Y_n^a(\theta_i,\mu) = P_n^0(\cos\theta_i),$$

$$Y_n^b(\theta_i,\mu) = P_n^1(\cos\theta_i)\cos\mu,$$

$$Y_n^c(\theta_i,\mu) = P_n^1(\cos\theta_i)\sin\mu.$$

Here $m=0$ for $k=a$ and $m=1$ for $k=b$ and c.

The constants f_{mn}^i and g_{mn}^i are evaluated using the normal velocity condition at the surface of the bubbles (4). The Legendre polynomials in the coordinate system centered at one bubble can be expressed in terms of those centered at the other bubble using the following expression derived by Hobson:[13]

$$\left(\frac{1}{r_i}\right)^{n+1} P_n^m(\cos\theta_i) = \left(\frac{1}{R}\right)^{n+1} \sum_{q=m}^{\infty} \binom{n+q}{q+m}$$
$$\times \left(\frac{r_{3-i}}{R}\right)^q P_q^m(\cos\theta_{3-i})$$
$$\text{for } r_{3-i} < R. \quad (10)$$

The constants f_{mn}^i and g_{mn}^i in (8) and (9) are expanded in a polynomial series in the parameter (a_i/R) as follows:

$$g_{mn}^i = \frac{1}{2} \sum_{p=0}^{\infty} K_{mnp}^i \left(\frac{a_i}{R}\right)^p, \quad (11a)$$

$$f_{mn}^i = \frac{1}{2} \sum_{p=0}^{\infty} L_{mnp}^i \left(\frac{a_i}{R}\right)^p. \quad (11b)$$

The condition on the normal velocity at the bubble surface (4) is used to obtain the constants K_{mnp}^i and L_{mnp}^i:

$$K_{mn0}^1 = (-1)^{m-1}\delta_{ln},$$

$$K_{mn0}^2 = s\delta_{ln}, \quad (12a)$$

$$K_{mnp}^1 = \left(\frac{n}{n+1}\right) \sum_{q=0}^{p-n-1} K_{mq(p-q-n-1)}^2 s^{p-n} \binom{n+q}{n+m},$$

$$K_{mnp}^2 = \left(\frac{n}{n+1}\right) \sum_{q=0}^{p-n-1} K_{mq(p-q-n-1)}^1$$
$$\times \left(\frac{1}{s}\right)^{p-n} \binom{n+q}{n+m},$$

$$L_{mn0}^1 = (-1)^{m-1}\delta_{ln},$$

$$L_{mn0}^2 = -s\delta_{ln}, \quad (12b)$$

$$L_{mnp}^1 = \left(\frac{n}{n+1}\right) \sum_{q=0}^{p-n-1} L_{mq(p-q-n-1)}^2 s^{p-n} \binom{n+q}{n+m},$$

$$L_{mnp}^2 = \left(\frac{n}{n+1}\right) \sum_{q=0}^{p-n-1} L_{mq(p-q-n-1)}^1$$
$$\times \left(\frac{1}{s}\right)^{p-n} \binom{n+q}{n+m}.$$

Here, s is the ratio of bubble sizes (a_2/a_1).

The leading-order correction to the velocity potential around a bubble due to the motion of a second bubble decreases as $(1/R)^3$ because of the following reason. The potential due to the motion of the second bubble decreases as $(1/r)^2$, and this can be expanded in a Taylor series about the center of the first bubble using (10). The leading term in this expansion, which decreases as $(1/R)^2$, is independent of spatial coordinates, and does not cause a disturbance to the fluid flow. Therefore, the leading correction to the potential which causes a velocity disturbance decreases as $(1/R)^3$.

The pressure on the surface of each bubble is calculated by substituting the expression for the potential, (9), (11), and (12), into the Bernoulli equation (3). This pressure is used in the force balance equation (5) to obtain six equations for the evolution of the bubble velocities:

$$\int_{A_i} \frac{\partial\phi}{\partial t} Y_1^k(\theta_i,\mu)dA_i + \int_{A_i} \frac{1}{2}u^2 Y_1^k(\theta_i,\mu)dA_i$$

$$+\frac{1}{\rho}\mathbf{F}_i\cdot\mathbf{e}_{ki}=0 \tag{13}$$

for $i=1,2$ and $k=a,b,c$. Note that the components of the unit normal in (13) have been written as spherical harmonics.

The time derivative of the velocity potential on the surface of bubble i is expressed in terms of the velocities of the bubbles and the distance between them:

$$\frac{\partial\phi}{\partial t} = \frac{\partial\phi}{\partial R}\frac{dR}{dt} + \sum_{k=a,b,c}\left(\frac{\partial\phi}{\partial V_k}\frac{dV_k}{dt} + \frac{\partial\phi}{\partial W_k}\frac{dW_k}{dt}\right) - \nabla\phi\cdot\mathbf{U}_i. \tag{14}$$

The last term in the expression above compensates for the motion of the spherical coordinate system with the bubble. Note that, whereas the spatial coordinates are defined in a coordinate system moving with the bubble, the velocities are relative to a fixed reference frame. Equations (1) and (14) were substituted into the force balance equations (13) to derive equations for the acceleration of the bubbles in the three coordinate directions. The surface integrals were first simplified by exploiting the symmetries of the Legendre polynomials about the coordinate axes, and then solved to obtain the following expressions for the accelerations of the bubbles correct to $O(a_i/R)^4$:

$$\frac{dU_{ia}}{dt} = \frac{9a_j^3}{2R^4}(U_{1b}U_{2b} + U_{1c}U_{2c} - 2U_{ja}^2) + \frac{\mathbf{F}_i\cdot\mathbf{e}_{ia}}{(2/3)\pi\rho a_i^3}, \tag{15a}$$

$$\frac{dU_{ik}}{dt} = \frac{9a_j^3}{2R^4}U_{ja}(U_{1k} + U_{2k}) + \frac{\mathbf{F}_i\cdot\mathbf{e}_{ik}}{(2/3)\pi\rho a_i^3},$$

$$\text{for } k=b,c. \tag{15b}$$

Here $j=3-i$. Note that the acceleration of the bubble due to the external force is equal to the force on the bubble divided by its added mass, which is half the mass of the fluid displaced by it. The external force $\mathbf{F}_i$ is the sum of the buoyancy and drag forces and is given by $[(\mathbf{U}_{it}-\mathbf{U}_i)/\tau_{vi}]$, where $\mathbf{U}_{it}$ is the terminal velocity, and τ_{vi} is the viscous relaxation time $[\rho a_i^2/(18\eta)]$. Although the first effect of bubble interactions on the fluid velocity decays as $(1/R^3)$ this term does not contribute to the bubble acceleration. The leading-order acceleration, which decays as $(1/R^4)$, results from the next correction to the fluid velocity.

III. INTERACTION BETWEEN BUBBLES OF DIFFERENT SIZES RISING DUE TO GRAVITY

Before proceeding to study the interactions between bubbles rising due to gravity, we briefly examine the validity of three approximations that are used in the calculation of the average properties of a suspension of bubbles in Sec. IV: (i) only the leading-order term in the expansion for the acceleration, which decreases as $(1/R)^4$, is retained in the

analysis; (ii) the effect of hydrodynamic interactions on the drag forces is neglected; and (iii) the bubbles are considered to be nondeformable.

The higher-order corrections in the expansion for the acceleration are difficult to calculate for the general case of two bubbles moving with arbitrary velocities. Kumaran[14] explicitly calculated these corrections for the simpler case of two bubbles approaching each other with equal velocities along their line of centers. Due to the symmetry of the configuration, the change in the velocities of the bubbles can be calculated using just the energy balance equation. In Kumaran's calculations, the bubbles were given an initial velocity of magnitude U_0 toward each other when their separation was $(10a_i)$, and terms up to $O(a_i/R)^{10}$ were retained in the expansion for the acceleration. As the bubbles approached each other, their velocities decreased to $0.83U_0$ due to the potential flow interaction when their surfaces touched. The error made by retaining only the leading-order term in the expansion was less than $0.015U_0$ at the point of contact. The asymptotic expansion could not be used when the gap between the surfaces became small compared to the bubble radius, because the series does not converge at small separations.

The effect of hydrodynamic interactions on the viscous drag was analyzed using the same configuration and including an additional viscous dissipation term for potential flow in the energy balance. The change in the viscous drag due to interactions was calculated correct to $O(a_i/R)^6$, and the error made by neglecting the higher-order terms was examined. It was found that including the effect of interactions on the drag force changed the velocity at the point of contact by 5% or less at Reynolds numbers of 100 and 200.

The effect of small deformations of the shape of the bubble was also studied using an energy balance formulation, taking into account the possibility of the conversion of kinetic energy of flow into potential energy for surface expansion. The bubbles were given a velocity U_0 when the distance between their centers was $10a_j$, and the difference in the velocity at contact between nondeformable and deformable bubbles was $0.02U_0$ at We$=0.5$, and $0.05U_0$ at We$=1.0$.

The above calculations indicate that the approximations used here will not cause significant errors when the Reynolds number is greater than 100 and the Weber number is less than 0.5. Note that these conclusions are only valid when the distance between the bubbles is comparable to the bubble radius. In addition, it should be noted that the analysis mentioned above did not take into account the effects of deformation and the change in the drag due to interactions on the center of mass motion, which may be significant.

In this paper, we analyze a bidisperse suspension of bubbles having a relatively large size difference, in which there are no collisions between the bubbles during an interaction. The interactions between bubbles of nearly equal size which do involve collisions are analyzed in Kumaran and Koch.[8] The interaction between a pair of bubbles in a dilute suspension is initiated by the approach of the larger
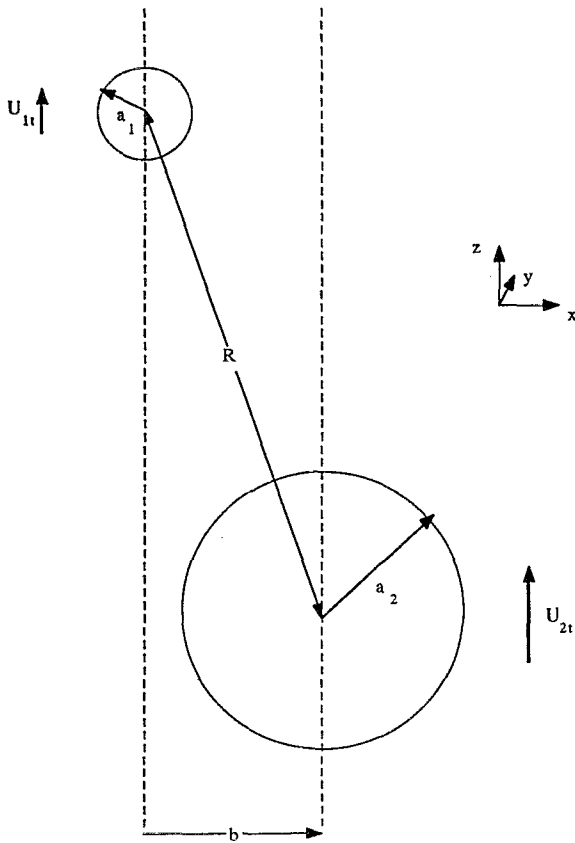
FIG. 2. Configuration of bubbles of different sizes rising due to gravity. In the initial configuration, the bubbles are rising at their terminal velocities, and the distance between their centers is large enough that the effect of interactions is negligible. The impact parameter b is the horizontal distance between their centers in the initial configuration.
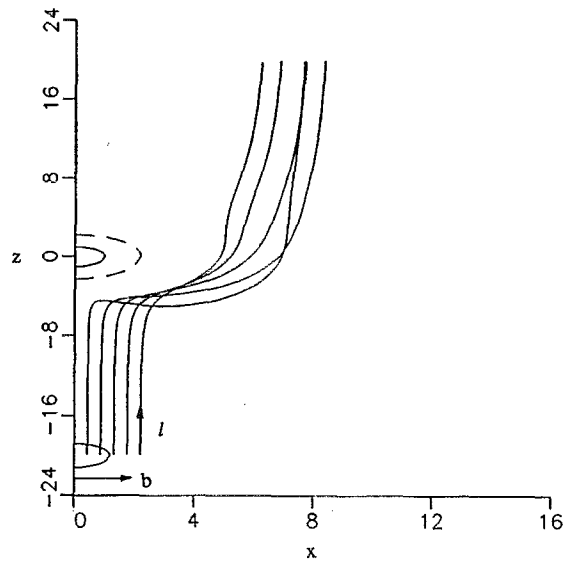

FIG. 3. Trajectories of bubbles of different sizes rising due to gravity for different values of the impact parameter. The position of the larger bubble is tracked in a reference frame moving with the smaller one. The radius of the larger bubble is 1.2 times that of the smaller one, and the Reynolds number, based on the radius and terminal velocity of the smaller bubble, is 200. In the initial configuration, the bubbles were rising at their terminal velocity, and vertical distance between the centers of the bubbles was 20 times the radius of the smaller one. All length scales are nondimensionalized by the radius of the smaller bubble.

bubble from below. This configuration is shown in Fig. 2, where the smaller bubble (bubble 1), which has a radius a_1 and a terminal velocity U_{1t}, is approached from below by a larger bubble (bubble 2) with radius a_2 and terminal velocity U_{2t}. Since the terminal velocity of bubble i is given by $[a_i^2 \rho g/(9\eta)]$, the ratio of the terminal velocities, (U_{2t}/U_{1t}), is s^2 if the ratio of the bubble radii, (a_2/a_1), is s. Initially, the distance between the bubbles is large enough that the effect of the interaction on the trajectories is negligible. However, the horizontal distance between the bubbles in the initial configuration, which is referred to as the impact parameter b, is comparable to the bubble radius. The trajectories are generated by numerically integrating the equations for the bubble accelerations (15), where $\mathbf{F}$ is the sum of the buoyancy and drag forces, and is given by $[(\mathbf{U}_{it}-\mathbf{U}_i)/\tau_{vi}]$. All lengths are nondimensionalized by a_1 and velocities by U_{1t}.

The trajectories of the larger bubble in a reference frame moving with the smaller bubble are shown in Figs. 3–7 for several values of the impact parameter b. In Fig. 3, the Reynolds number Re_1 is 200, the size ratio is 1.2, and the positions of the bubbles are $(0,0)$ and $(b,-20)$ in the initial configuration. Here, the Reynolds number Re_i is based on the size and terminal velocity of bubble i. In Fig. 4, the size ratio is maintained at 1.2, but the Reynolds

number is reduced to 100. At a lower Reynolds number the bubbles relax to their terminal velocity faster due to viscous drag, and the displacement of the bubbles is smaller. The effect of the variation of the size ratio at a Reynolds
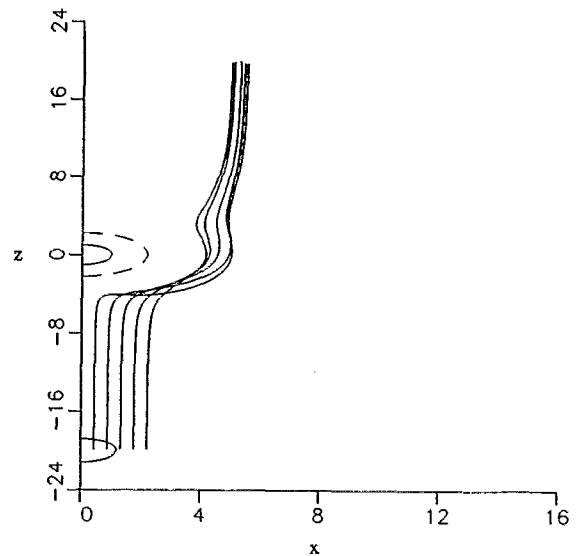

FIG. 4. Trajectories of bubbles of different sizes rising due to gravity for different values of the impact parameter. The position of the larger bubble is tracked in a reference frame moving with the smaller one. The radius of the larger bubble is 1.5 times that of the smaller one, and the Reynolds number, based on the radius and terminal velocity of the smaller bubble, is 200.
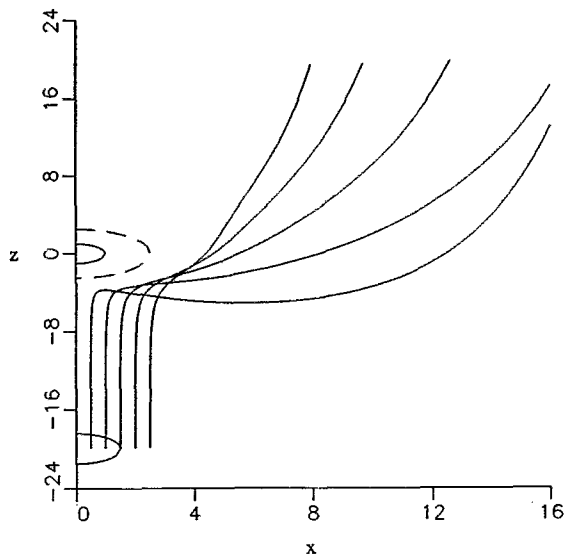
FIG. 5. Trajectories of bubbles of different sizes rising due to gravity for different values of the impact parameter. The position of the larger bubble is tracked in a reference frame moving with the smaller one. The radius of the larger bubble is 1.2 times that of the smaller one, and the Reynolds number, based on the radius and terminal velocity of the smaller bubble, is 100.
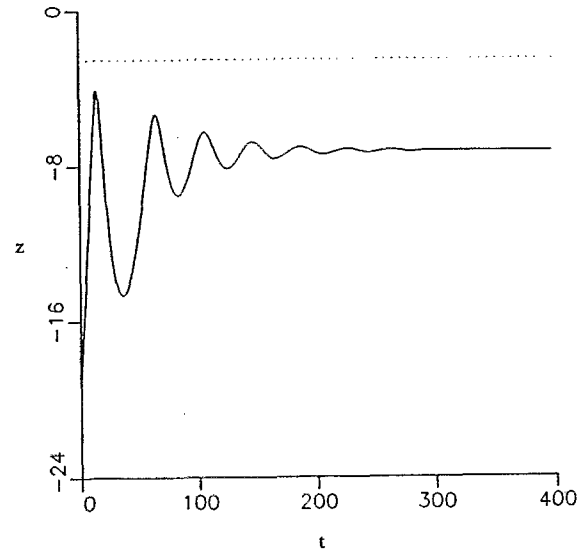

FIG. 6. The vertical distance between a pair of bubbles of different sizes rising along the same vertical line, as a function of time. The radius of the larger bubble is 1.2 times that of the smaller one, and the Reynolds number based on the radius and terminal velocity of the smaller bubble is 200. In the initial configuration, the bubbles were rising at their terminal velocities, and the distance between their centers was 20 times the radius of the smaller bubble.

number of 200 can be seen by comparing Fig. 3 and Fig. 5, where the larger bubble is 1.5 times bigger than the smaller one. As the size ratio is increased, the displacement of the smaller bubble increases due to an increase in the inertia of the fluid flow driven by the larger one. The displacements of the bubbles are large compared to their radii because the time required for a bubble to relax to its terminal velocity is $O(\text{Re}/18)$ when scaled by the radius and terminal velocity of the bubble.

The surface indicated by the broken line around bubble 1 is a hemisphere of radius $(s+1)$; if the center of bubble 2 is on this hemisphere, the surfaces of the bubbles touch. As can be seen from the figures, the surfaces of the bubbles never come into contact. Even when the bubbles are initially in the same vertical line ($b=0$), the relative velocity decreases to zero as they approach each other. This is shown in Fig. 6, which is a plot of the vertical distance between the bubbles as a function of time, when the larger bubble is directly below the smaller one. The size ratio is 1.5, the Reynolds number based on the size and terminal velocity of the smaller bubble is 200, and the vertical displacement of bubble 2 is traced in a reference frame moving with bubble 1. The potential flow interaction between the bubbles is repulsive for vertically oriented separations. The combined effects of the attractive buoyancy force, the repulsive potential flow interactions, and the added mass inertia, lead to an oscillation of the separation, which is eventually damped due to viscous drag. The separation and velocity of the bubbles at steady state for this configuration can be calculated from the equation for the acceleration (15). The rise velocity U is

$$U=\left(\frac{s^3+1}{s+1}\right) \tag{16a}$$

and the distance between the centers of the bubbles at steady state is

$$R=\left(\frac{\text{Re}\,s^3U^2}{U-1}\right)^{1/4}. \tag{16b}$$

In the above calculation, we have neglected the effect of the wake below the smaller bubble. For an isolated bubble rising in a liquid, it was shown by Moore[1] that the near wake ($R \sim a$) has a thickness of $O(\text{Re}^{-1/4})$, and the perturbation to the velocity due to viscous forces in the wake is $O(\text{Re}^{-1/2})$. The viscous forces in the far wake ($R \gg a$) are small compared to the inertial forces at downstream distances less than ($a\,\text{Re}^{1/2}$), and therefore we neglect the effect of the wake in the limit $\text{Re} \gg 1$. Moore showed that the first correction to the drag force on the bubble due to wake effects was ($-2.211\,\text{Re}^{-1/2}$) times the leading-order drag force. Subsequently, Harper[15] calculated the higher-order correction to the drag force of a bubble when it rises in the wake of another bubble of the same size, obtaining ($-4.345\,\text{Re}^{-1/2}$) times the leading-order drag force. Thus, the variation in the drag force due to wake effects is small for $\text{Re} \gg 1$.

When the size ratio s is much smaller than 1, the bubbles "collide" with each other repeatedly during the interaction. Here we have used "collide" to indicate that a calculation based on nondeformable bubbles gives the result that the bubbles touch while still moving at a finite relative velocity. Figure 7 shows the trajectory of the smaller bubble (bubble 1) in a reference frame moving with the larger
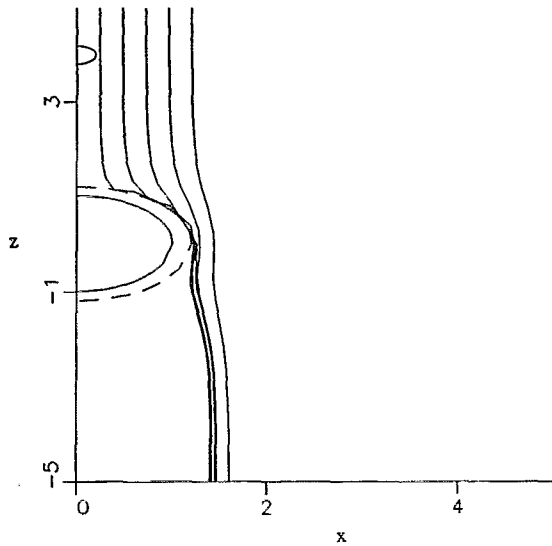
FIG. 7. Trajectories of bubbles of different sizes rising due to gravity. The position of the smaller bubble is tracked in a reference frame moving with the larger one. The ratio of the radii of the bubbles is 0.2 and the Reynolds number, based on the radius and terminal velocity of the larger bubble, is 200. In the initial configuration, the bubbles were rising at their terminal velocity, and the distance between their centers was 20 times the radius of the larger bubble.

bubble (bubble 2), where the size ratio is 0.2 and the Reynolds number of the larger one is 200. The bubbles collided for $(a_1/a_2) < 0.233$ at $Re_2 = 200$ and $(a_1/a_2) < 0.365$ at $Re_2 = 100$.

However, it should be noted that since Re_1 is $O(a_1/a_2)^3$ smaller than Re_2, the Reynolds number of the smaller bubble is $O(1)$, and the potential flow equations cannot be used to describe its motion. Although the trajectories in Fig. 7 are not quantitatively accurate for low Reynolds number, it is of interest to know whether bubble coalescence may still be expected. For $Re_1 \ll 1$ and $a_1 \ll a_2$, the small bubble will approximately follow a streamline in the flow relative to the large bubble until the separation is $O(a_1)$. The streamlines converge toward the surface of the large bubble on its upstream side, and the flow drives the small bubble into the surface. The lubrication analysis of Davis et al.[16] indicates that the lubrication forces are too weak to slow the coalescence process significantly at low Reynolds number. Thus, the coalescence time is much smaller than the time it takes for one bubble to translate past the other.

The result of the interaction between a pair of bubbles whose size ratio is between 0.9 and 1.1 is qualitatively different from that discussed in this section. The bubbles approach each other along the horizontal plane and collide repeatedly. This type of interaction is discussed in detail in Kumaran and Koch,[8] and from the scaling of the pressure in the gap between the bubbles, we expect coalescence to occur in finite time. This difference can be qualitatively explained as follows. Potential flow interactions cause vertically oriented bubbles to repel, and horizontally oriented bubbles to attract. Thus, bubbles of equal size, which have equal terminal velocities, come together along the horizon-

tal plane and collide with a finite velocity toward each other. The interaction between bubbles of different sizes is driven by the difference in their terminal velocities, and takes place within the finite time period required for the bubbles to translate past each other. The interaction is strongest when the distance between the bubbles is small and the orientation of the line of centers is closer to the vertical, and in this configuration the interaction is repulsive. Due to this repulsion, the horizontal distance between them increases as the larger bubble translates past the smaller one. The bubbles do experience some attraction farther downstream along the trajectory when the line joining their centers is oriented closer to the horizontal (see Figs. 3–5). However, this attraction is insufficient to capture them in closed trajectories before they have translated past each other.

IV. AVERAGE PROPERTIES OF A BIDISPERSE SUSPENSION

In this section, we use pair averaging to determine the properties of a bidisperse suspension of bubbles. The dynamics of the suspension is governed by two time scales: (i) the interaction time, τ_c, which is the time between successive interactions of a bubble and (ii) the viscous relaxation time, τ_{vi}, which is the time it takes a bubble of species i to relax to its terminal velocity after an interaction. The viscous relaxation time is the ratio of the drag coefficient and the added mass of the bubbles:

$$\tau_{vi} = \frac{\rho a_i^2}{18 \eta U_{it}} = \frac{Re_i}{18} \frac{a_i}{U_{it}}. \tag{17}$$

The time between successive interactions is the inverse of the interaction frequency:

$$\tau_c = 1/\{n_i [\pi(a_1 + a_2)^2] U_{it}\}. \tag{18}$$

The ratio of the viscous relaxation time to the interaction time, (τ_{vi}/τ_c), is $O(V Re/18)$. Here V is the volume fraction of the bubbles and Re is the Reynolds number based on the bubble radius and terminal velocity. Thus, the bubbles relax to their terminal velocities between successive collisions in the limit $V \ll 18/Re$, and the pair averaging procedure is valid in this limit.

In a polydisperse suspension, the frequency of interactions between bubbles of two different sizes is inversely proportional to the difference in their terminal velocities in the limit $V \ll 18/Re$. Interactions between bubbles of nearly equal size, which lead to coalescence, are analyzed in Kumaran and Koch.[8] The interactions between bubbles having a larger size difference, which occur with a higher frequency, do not lead to coalescence. However, these interactions cause velocity fluctuations and a spatial transport of bubbles in the suspension. The mean-square fluctuating velocity and diffusion coefficients in the suspension are calculated in this section. For simplicity, we analyze a bidisperse suspension in which the bubbles have two distinct sizes, but the procedure can be quite easily modified for calculating the fluctuating velocities and diffusion co-

efficients in a polydisperse suspension. The latter would involve one additional step, which is an average over the size distribution in the suspension.

If we neglect interactions in the leading-order approximation, the bubbles of the two species rise at their respective terminal velocities. A perturbation analysis about this base state is used to calculate the first correction to the mean and mean-square velocities in a spatially uniform suspension in Sec. IV A. The diffusion coefficients in a nonuniform suspension are calculated in Sec. IV B.

A. Mean and mean-square velocities in a uniform suspension

In this section, we calculate the averages of the following quantities in a uniform suspension: (1) the difference between the mean velocity and terminal velocity, $(U_{iz}-U_{it})$; (ii) the square of the fluctuating velocity in the vertical direction, $(U_{iz}-U_{it})^2$; and (iii) the square of the fluctuating velocity along any direction in the horizontal plane, U_{ir}^2. Note that these velocities are nonzero only during an interaction. The moments are calculated by doing an ensemble average over all relative configurations of the bubbles during an interaction:

$$\langle\beta_i\rangle=\int_b\int_l\beta_i[\mathbf{U}_i(b,l)]P_j(b,l)2\pi b\,db\,dl, \qquad (19)$$

where b is the impact parameter of the trajectory of the bubble of the other species j and l is the coordinate of the bubble along this trajectory, as shown in Fig. 3. Here $\beta_i[\mathbf{U}_i(b,l)]$ is the value of β_i due to the presence of the second bubble (b,l) moving with a velocity $\mathbf{U}_j$. The conditional $P_j(b,l)$ is the probability of finding the bubble of species j which has traveled along the trajectory having impact parameter b and is located at (b,l). If the time scale of the interaction is large compared to the viscous relaxation time, the velocity fluctuation decreases as $(1/R)^4$. Since the moments calculated here are nonzero only for the period of the interaction, the integral in (19), evaluated over all space, is convergent.

The conditional probability, $P_j(b,l)$, is equal to the number density of bubbles of species j, n_j, when the distance between the bubbles is large. As the bubbles come closer together, however, the interaction between the bubbles causes a change in this probability. The divergence of the flux of the conditional probability is zero. Since the impact parameter does not change during an interaction, this reduces to the condition that the flux, $(|\mathbf{U}_i-\mathbf{U}_j|P_j)$, along the trajectory is independent of l. Initially, the distance between the bubbles is large enough that the effect of interactions is negligible. In this configuration, the probability of finding a bubble of species j in the differential volume $d\mathbf{x}$ is $(n_j\,d\mathbf{x})$, and the bubbles are moving at their respective terminal velocities. Therefore at any point along the trajectory, the probability of finding a bubble of species j is given by

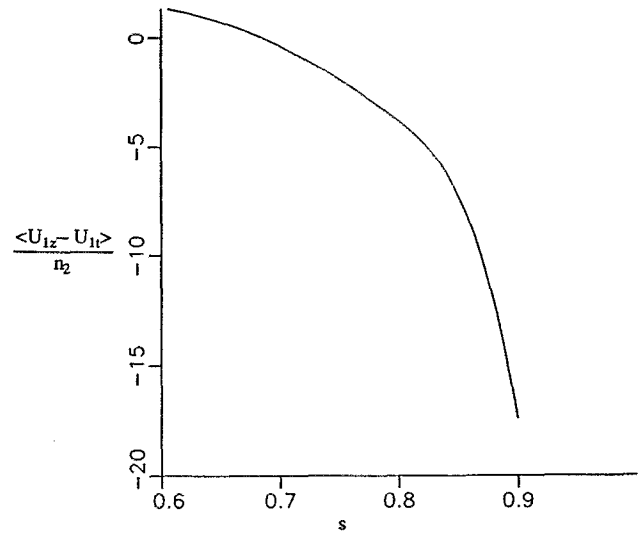$$P_j(b,l)=n_j\frac{(U_{it}-U_{jt})}{|\mathbf{U}_i-\mathbf{U}_j|}. \qquad (20)$$

FIG. 8. $[\langle(U_{1z}-U_{1t})\rangle/n_2]$ plotted as a function of size ratio, $s=(a_2/a_1)$. The Reynolds number based on the radius and terminal velocity of species 1 is 200.

The ensemble averages are calculated using a finite-difference scheme in a reference frame moving with the bubble of species i. The trajectory of a bubble having an impact parameter b is divided into a finite number of intervals of length $\Delta l=(|\mathbf{U}_i-\mathbf{U}_j|\Delta t)$, where Δt is a small time interval. From (20), the number of bubbles of species j in each differential volume is $[n_j2\pi b\,db(U_{it}-U_{jt})\Delta t]$. The integrand in (19) is weighted by this probability and numerically integrated over the b and l coordinates to give the ensemble average $\langle\beta_i\rangle$. This ensemble average is proportional to n_j, the number density of the other species j, since the probability $P_j(b,l)$ is proportional to n_j. Figures 8–11 show the variation of $(\langle\beta_1\rangle/n_2)$ as a function of Reynolds number and size ratio.

Figure 8 is a plot of $(\langle U_{1z}-U_{1t}\rangle/n_2)$ as a function of size ratio at a Reynolds number of 200. At a size ratio between about 0.7 and 0.9, the interaction slows down the larger bubble, and the difference between the mean velocity and the terminal velocity is negative. As the size ratio is decreased, however, the average effect of interactions results in an increase in the velocity of the larger species. This rather surprising result can be qualitatively explained as follows. If we assume the two bubbles are traveling at their terminal velocities, the acceleration of the larger bubble in the vertical direction is given by

$$\frac{dU_{1z}}{dt}=\frac{9}{2}\frac{U_{1t}^2}{a_1}\left(\frac{a_1}{R}\right)^4 s^5[(s^2+2)\sin^2\theta-2s^2\cos^2\theta]. \qquad (21)$$

This interaction is repulsive when the azimuthal angle of the line joining the centers of the bubbles satisfies the following criterion:
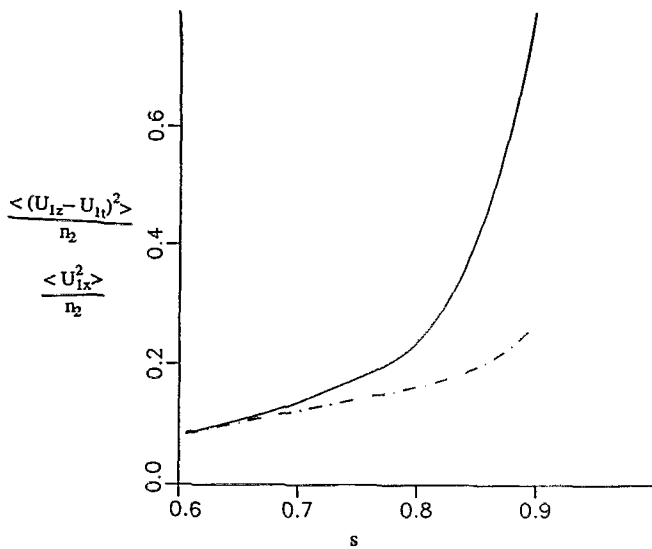
$$\tan^2\theta<2s^2/(s^2+2). \qquad (22)$$

FIG. 9. $[\langle(U_{1z}-U_{1t})^2\rangle/n_2]$ and $(\langle U_{1r}^2\rangle/n_2)$ as a function of size ratio, $s=(a_2/a_1)$. The Reynolds number based on the radius and terminal velocity of species 1 is 200. ———: $[\langle(U_{1z}-U_{1t})^2\rangle/n_2]$; —·—: $(\langle U_{1r}^2\rangle/n_2)$.

FIG. 10. $[\langle(U_{1z}-U_{1t})\rangle/n_2]$ as a function of the Reynolds number, Re, based on the radius and terminal velocity of species 1. The size ratio, (a_2/a_1), is 1.25.

As the size ratio s is decreased the domain of repulsion decreases and the mean velocity of the larger species increases and eventually becomes greater than its terminal velocity.

The quantities $[\langle(U_{1z}-U_{1t})^2\rangle/n_2]$ and $(\langle U_{1r}^2\rangle/n_2)$ are plotted as a function of size ratio for a Reynolds number of 200 in Fig. 9. The mean-square velocity fluctuations in the vertical direction are greater than those in the horizontal direction for a size ratio greater than about 0.7. For smaller size ratios, the two variances are approximately equal. There is an increase in the velocity moments as the size ratio approaches 1 because the difference in the terminal velocities decreases, and the bubbles interact for longer periods of time. Note that the graphs have not been extended beyond a size ratio greater than about 0.9. The interactions between bubbles having a greater size ratio result in collisions and coalescence, and this results in a change in the size distribution of the suspension. This phenomenon is analyzed in another publication.[7] However, the properties remain finite as we approach the critical size ratio at which collisions occur.

The quantity $(\langle U_{1z}-U_{1t}\rangle/n_2)$ is shown as a function of Reynolds number for a size ratio of 1.25 in Fig. 10, and the quantities $[\langle(U_{1z}-U_{1t})^2\rangle/n_2]$ and $(\langle U_{1r}^2\rangle/n_2)$ are plotted for the same size ratio in Fig. 11. These three quantities increase linearly at large Reynolds numbers, since the viscous relaxation time is proportional to (Re/18). The mean-square velocity in the vertical direction is about 1.2 to 1.5 times that in the horizontal direction. In the above figures, the number density n_2 is nondimensionalized by $(1/a_2^3)$. In the limit of small volume fraction, the mean and mean-square velocities are proportional to the product of the abscissas in the figures and the volume fraction.
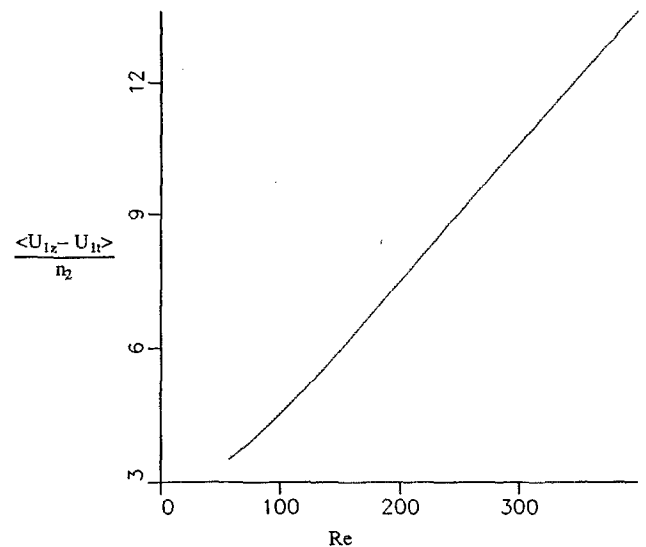
B. Diffusion of bubbles in a nonuniform suspension

The interaction between bubbles causes a spatial transport in a reference frame moving at their respective terminal velocities, and this drives a flux in a nonuniform suspension. In this section, we use ensemble averaging to calculate diffusion coefficients that relate the flux to the gradients in the number densities of the bubbles as follows:

$$J_x^i = D_x^{ij}\frac{\partial n_j}{\partial x}, \quad J_z^i = D_z^{ij}\frac{\partial n_j}{\partial z}. \tag{23}$$

Here J_x^i and J_z^i are the flux of bubbles of species i in the horizontal and vertical directions, respectively, and D_x^{ij} and
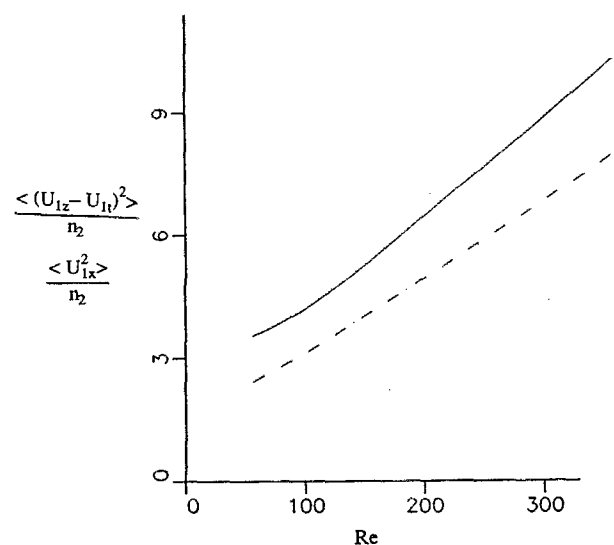

FIG. 11. $[\langle(U_{1z}-U_{1t})^2\rangle/n_2]$ and $(\langle U_{1r}^2\rangle/n_2)$ as a function of the Reynolds number, Re, based on the radius and terminal velocity of species 1. The size ratio, (a_2/a_1), is 1.25. ———: $[\langle(U_{1z}-U_{1t})^2\rangle/n_2]$; —·—: $(\langle U_{1r}^2\rangle/n_2)$.

D_z^{ij} are the diffusion coefficients. Note that in this analysis we include cross-diffusion coefficients which relate the flux of species i to gradients in the number density of species j. This flux results from the dependence of the interaction frequency of bubbles of species i on n_j.

The diffusion coefficients scale as (λ_i^2/τ_c), where λ_i, the transport length, is the displacement of the bubble during an interaction. To calculate a diffusion coefficient that depends only on the instantaneous number density gradient, we need to satisfy two conditions: (i) the transport length λ_i should be small compared to the length scale of the number density gradients L, i.e., $\lambda_i \ll L$; and (ii) the time scale of the variation of number density gradients should be large compared to the time period of an interaction, which is the viscous relaxation time, τ_{vi}. The transport length λ_i scales as $(U_{it}\tau_{vi})$, since the perturbation to the velocity of the bubble during an interaction is $O(U_{it})$ and the time it takes a bubble to relax to its terminal velocity is $O(\tau_{vi})$. Therefore, λ_i is $O(a_i \operatorname{Re}_i/18)$, which is about ten times the bubbles' radius for Reynolds numbers of $O(200)$, and the first condition is satisfied for $L \gg 10a_i$. A characteristic time scale for the number density variations is $(L^2\tau_c/\lambda_i^2)$, which is large compared to τ_{vi} for $L/\lambda_i \gg V \operatorname{Re}_i/18$. In the limit $V \operatorname{Re}_i/18 \ll 1$ the first condition is more stringent, and this analysis is valid in the limit $(L/a_i \gg \operatorname{Re}_i/18)$.

An interaction causes a horizontal displacement x_{ci} and a vertical displacement z_{ci} of the bubble of species i in a reference frame moving at its terminal velocity. These displacements are functions of the impact parameter of the interaction, the size ratio of the bubbles, and the Reynolds number.

To calculate the horizontal flux, consider a vertical plane at $x=0$, across which the variation in the number density is given by the following linearized equation over length scales of $O(\lambda_i)$:

$$n_i(x) = n_i(0) + n_i'(0)x. \tag{24}$$

The transport of bubbles across this plane is caused by interactions in a region of width X_{ci} on either side of the plane, where X_{ci} is the maximum deflection caused by the interactions. Consider a differential length $d\xi$ about the point $x=\xi$ in this region. The deflection of a bubble in the x direction due to an interaction with impact parameter b is given by $[x_{ci}(b)\cos\mu]$. Here $x_{ci}(b)$ is the magnitude of the deflection due to an interaction with impact parameter b, and μ is the meridional angle, which is the angle between the projection into the x-y plane of the line joining the centers of the bubbles and the x axis. The number of interactions per unit area in the y-z plane per unit time in the region ξ to $\xi+d\xi$, having an impact parameter in the interval db about b and a polar angle in the interval $d\mu$ about μ, is given by

number of interactions/area/time

$$= n_1(\xi)n_2(\xi)b\,db\,d\mu\,d\xi|U_{2t}-U_{1t}|, \tag{25}$$

where the number densities $n_1(\xi)$ and $n_2(\xi)$ are given by (24). For an impact parameter b, the interaction results in

a transport across $x=0$ if the deflection $(x_{ci}\cos\mu)$ is greater in magnitude than ξ, and directed toward the $x=0$ plane. To calculate the net flux, we integrate (25) in the ξ coordinate from 0 to $(-x_{ci}\cos\mu)$, in the μ coordinate from 0 to 2π, and over all values of the impact parameter b,

$$J_x^i = \int_b \int_{\mu=0}^{2\pi} \int_{\xi=-x_{ci}\cos\mu}^{0} n_1(\xi)n_2(\xi)|U_{1t}-U_{2t}|$$

$$\times d\xi\,d\mu\,b\,db$$

$$= -\frac{\pi}{2}[n_1(0)n_2' + n_2(0)n_1']|U_{1t}-U_{2t}|\int_b x_{ci}^2 b\,db. \tag{26}$$

In the above expression, μ is in the intervals $(0,\pi/2)$ and $(3\pi/2,2\pi)$ for bubbles transported in the positive x direction, and in the interval $(\pi/2,3\pi/2)$ for bubbles transported in the negative x direction. The diffusion coefficient calculated from the above equation is

$$D_x^{ij} = \frac{\pi}{2}|U_{1t}-U_{2t}|n_{3-j}(0)\int_b x_{ci}^2 b\,db. \tag{27}$$

The diffusion coefficient in the vertical direction is calculated in a similar manner. Consider a horizontal plane at $z=0$ in the suspension which is moving at the terminal velocity of species i. The number density across this plane is assumed to be linear in the z coordinate over length scales comparable to the transport length λ_i:

$$n_i = n_i(0) + n_i'(0)z. \tag{28}$$

There is a flux of bubbles due to interactions in the region within a distance Z_{ci} about the plane $z=0$, where Z_{ci} is the maximum deflection due to an interaction. The flux is independent of the meridional angle μ in this case, since the configuration is axisymmetric. The frequency of interactions in an interval $d\zeta$ at a distance ζ below $z=0$, per unit area in the x-y plane per unit time, that have an impact parameter in the differential width db about b, is given by

number of interactions/area/time

$$= n_1(\zeta)n_2(\zeta)|U_{1t}-U_{2t}|(2\pi b\,db)d\zeta. \tag{29}$$

The above interaction causes a flux through the surface $z=0$ if the deflection z_{ci} is greater than ζ. Therefore, the total flux is calculated by integrating the above expression in z from 0 to z_{ci} and over all values of b:

$$J_z^i = \int_b \int_{\zeta=-z_{ci}}^{0} n_1(\zeta)n_2(\zeta)|U_{1t}-U_{2t}|(2\pi b)d\zeta\,db$$

$$= n_1(0)n_2(0)|U_{1t}-U_{2t}|\int_b z_c(2\pi b)db$$

$$-\pi[n_1(0)n_2' + n_2(0)n_1']|U_{1t}-U_{2t}|\int_b z_{ci}^2 b\,db. \tag{30}$$

The first term in the above expression is a flux in a uniform suspension due to the difference between the mean velocity and the terminal velocity, and is the same as that calcu-
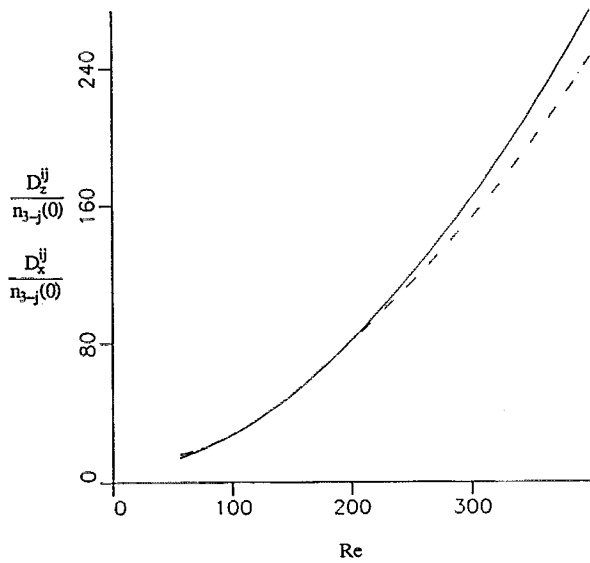
1132   Phys. Fluids A, Vol. 5, No. 5, May 1993

V. Kumaran and D. L. Koch   1132

FIG. 12. $[D_x^{ij}/n_{3-j}(0)]$ and $[D_z^{ij}/n_{3-j}(0)]$ as a function of the Reynolds number, Re, based on the radius and terminal velocity of species 1. The size ratio, (a_2/a_1), is 1.25. $-\cdot-$: $[D_x^{ij}/n_{3-j}(0)]$; ———: $[D_z^{ij}/n_{3-j}(0)]$.

lated in Sec. IV A. The second term represents the diffusion in a nonuniform suspension, and the coefficient of diffusion calculated from this term is

$$D_z^{ij} = \pi n_{3-j}(0) \, |U_{1t} - U_{2t}| \int_b z_{ct}^2 b \, db. \tag{31}$$

From (27) and (31), D_x^{ij} and D_z^{ij} are proportional to the number density $n_{3-j}(0)$. Here $D_x^{ij}/n_{3-j}(0)$ and $D_z^{ij}/n_{3-j}(0)$ are shown as a function of Reynolds number for $(a_{3-i}/a_i) = 1.25$ in Fig. 12. Here, the number density $n_{3-j}(0)$ has been nondimensionalized by $(a_{3-j})^3$. The diffusion coefficients are quadratic functions of Re at high Reynolds numbers, and the coefficients in the horizontal and vertical directions are about equal for a size ratio of 1.25. In Figs. 13 and 14, $D_x^{ij}/n_{3-j}(0)$ and $D_z^{ij}/n_{3-j}(0)$ are plotted as a function of size ratio at a Reynolds number of 200. As expected, the diffusion coefficients increase as the size ratio increases. The diffusion coefficients in the two directions are almost equal for $(a_{3-i}/a_i) > 1.1$, and the diffusion coefficient in the vertical direction is greater than that in the horizontal direction for $(a_{3-i}/a_i) < 0.9$. The diffusion coefficients have not been calculated for values of the size ratio between 1.1 and 0.9, because interaction between bubbles in this size range results in coalescence. Since the diffusion coefficients are always positive, interactions may be expected to have a damping effect on number density variations.

V. CONCLUSIONS

The interactions between a pair of unequal sized nondeformable bubbles in potential flow were studied in Sec. II. A perturbation solution in the parameter (a_i/R) was obtained, and it was shown that the leading-order bubble acceleration decreases as $(a_i/R)^4$ at large separations. While calculating the trajectories of bubbles rising due to
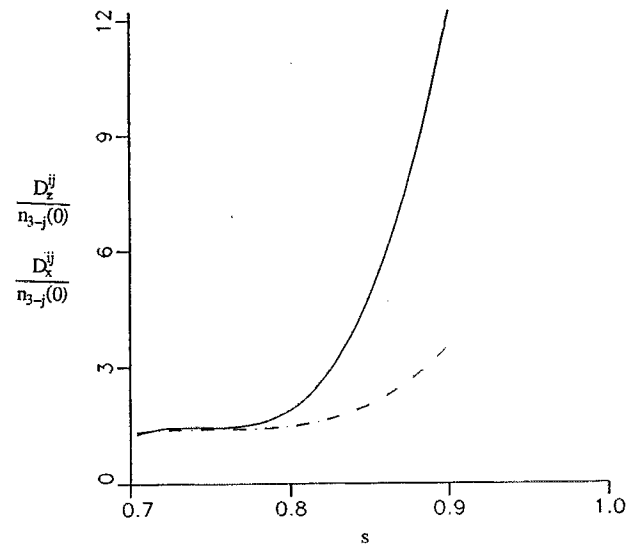

FIG. 13. $[D_x^{ij}/n_{3-j}(0)]$ and $[D_z^{ij}/n_{3-j}(0)]$ as a function of size ratio $s = (a_2/a_1)$. The Reynolds number based on the radius and terminal velocity of species 1 is 200. $-\cdot-$: $[D_x^{ij}/n_{3-j}(0)]$; ———: $[D_z^{ij}/n_{3-j}(0)]$.

gravity, the bubbles were assumed to be nondeformable, only the leading-order term in the expression for the acceleration due to the potential flow interaction was retained, and the effect of the interaction on the bubble drag was neglected. A brief summary on the previous work on the validity of these approximations was provided at the beginning of Sec. III.

In Sec. III, we analyzed the interaction between a pair of bubbles rising due to gravity, when the size ratio of the bubbles was greater than about 1.1. The surfaces of the bubbles did not come into contact during the interaction, and therefore there was no possibility of coalescence. There are repeated collisions between bubbles having a size ratio
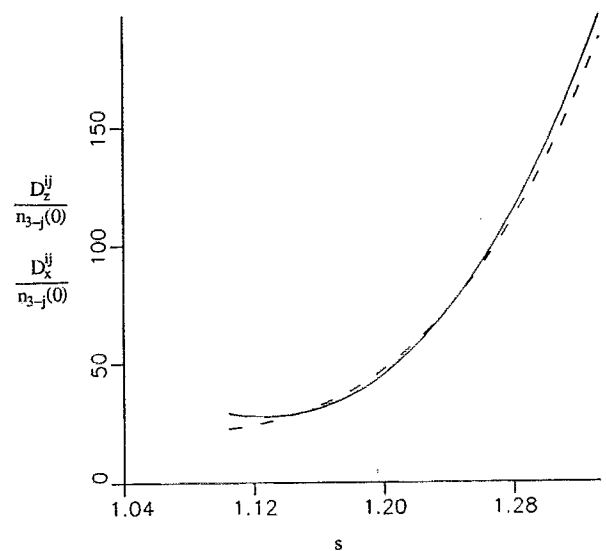

FIG. 14. $[D_x^{ij}/n_{3-j}(0)]$ and $[D_z^{ij}/n_{3-j}(0)]$ as a function of size ratio $s = (a_2/a_1)$. The Reynolds number based on the radius and terminal velocity of species 1 is 200. $-\cdot-$: $[D_x^{ij}/n_{3-j}(0)]$; ———: $[D_z^{ij}/n_{3-j}(0)]$.

between 0.9 and 1.1 at a Reynolds number of 100, and between bubbles having a size ratio between 0.93 and 1.07 at a Reynolds number of 200. The analysis of this interaction is presented in Kumaran and Koch.[8] Collisions were also observed when the larger bubble was rising at Re = 200 and the smaller bubble was less than 0.233 times the larger one. In this case, the Reynolds number based on the smaller bubble is not large enough to justify a potential flow approximation, but it was conjectured that coalescence would occur.

The average properties of a bidisperse suspension of bubbles rising due to gravity were calculated by performing an ensemble average over pair interactions in Sec. IV. An ensemble averaging procedure, which takes into account the change in the pair distribution due to interactions, was used to calculate the mean and mean-square velocities in a uniform suspension. The interactions cause a spatial displacement of the bubbles in a reference frame moving at the terminal velocity, and this drives a flux of bubbles in a nonuniform suspension. The diffusion coefficients in a nonuniform suspension were calculated by relating the spatial displacement of the bubble to the impact parameter of the interaction. Since the diffusion coefficients are positive, the interactions drive a flux of bubbles from regions of higher number density to regions of lower number density. This mechanism tends to damp out number density variations, and has a stabilizing influence on a uniform suspension.

ACKNOWLEDGMENT

[1] D. W. Moore, "The boundary layer on a spherical gas bubble," J. Fluid Mech. 16, 161 (1963).

[2] V. G. Levich, Physiochemical Hydrodynamics (Prentice–Hall, Englewood Cliffs, NJ, 1962).

[3] D. W. Moore, "The velocity of rise of distorted gas bubbles in a liquid of small viscosity," J. Fluid Mech. 23, 749 (1965).

[4] G. Ryskin and L. G. Leal, "Numerical solution of free boundary problems in fluid mechanics. Part 2. Buoyancy driven motion of a gas bubble through a quiescent liquid," J. Fluid Mech. 148, 19 (1984).

[5] A. Biesheuvel and L. van Wijngaarden, "The motion of pairs of gas bubbles in a liquid," J. Eng. Math. 16, 349 (1982).

[6] J. B. W. Kok, "Dynamics of gas bubbles moving through liquid," Ph.D. thesis, Technological University Twente, Enschede, The Netherlands, 1989.

[7] J. B. W. Kok, "Collision dynamics of bubbles pairs moving through a perfect fluid," Appl. Sci. Res. (in press).

[8] V. Kumaran and D. L. Koch, "The rate of coalescence in a suspension of high Reynolds number, low Weber number bubbles," Phys. Fluids A 5, 1135 (1993).

[9] D. A. Drew, "Mathematical modeling of two-phase flows," Annu. Rev. Fluid Mech. 15, 261 (1983).

[10] G. B. Wallis, One Dimensional Two-Phase Flow (McGraw-Hill, New York, 1969).

[11] L. van Wijngaarden and A. Biesheuvel, "Voidage waves in bubbly flows," in Transient Phenomena in Multiphase Flows, edited by N. H. Afgan (Hemisphere, New York, 1988).

[12] A. S. Sangani, D. Z. Zhang, and A. Prosperetti, "The added mass, Basset, and viscous drag coefficients in nondilute bubbly liquids undergoing small amplitude oscillatory motion," Phys. Fluids A 3, 2955 (1991).

[13] E. W. Hobson, The Theory of Spherical and Ellipsoidal Harmonics (Cambridge U.P., Cambridge, 1965).

[14] V. Kumaran, "Dynamics of suspensions with significant inertial effects," Ph.D. thesis, Cornell University, Ithaca, NY, 1992.

[15] J. F. Harper, "On bubbles rising in line at large Reynolds numbers," J. Fluid Mech. 41, 751 (1970).

[16] R. H. Davis, J. H. Schonerg, and J. A. Rallison, "The lubrication force between two viscous drops," Phys. Fluids A 1, 77 (1989).